Energy Decomposition Scheme Based on the Generalized Kohn–Sham Scheme

ARTICLE *in* THE JOURNAL OF PHYSICAL CHEMISTRY A · MARCH 2014

Impact Factor: 2.69 · DOI: 10.1021/jp500405s · Source: PubMed

4 AUTHORS, INCLUDING:

Peifeng Su
Xiamen University
22 PUBLICATIONS **605** CITATIONS
SEE PROFILE

Wei Wu
Xiamen University
102 PUBLICATIONS **2,038** CITATIONS
SEE PROFILE

THE JOURNAL OF PHYSICAL CHEMISTRY A

Article

pubs.acs.org/JPCA

Energy Decomposition Scheme Based on the Generalized Kohn−Sham Scheme

Peifeng Su,* Zhen Jiang, Zuochang Chen, and Wei Wu

The State Key Laboratory of Physical Chemistry of Solid Surfaces, Fujian Provincial Key Laboratory of Theoretical and Computational Chemistry, and College of Chemistry and Chemical Engineering, Xiamen University, Xiamen, Fujian 361005, China

ABSTRACT: In this paper, a new energy decomposition analysis scheme based on the generalized Kohn−Sham (GKS) and the localized molecular orbital energy decomposition analysis (LMO-EDA) scheme, named GKS-EDA, is proposed. The GKS-EDA scheme has a wide range of DFT functional adaptability compared to LMO-EDA. In the GKS-EDA scheme, the exchange, repulsion, and polarization terms are determined by DFT orbitals; the correlation term is defined as the difference of the GKS correlation energy from monomers to supermolecule. Using the new definition, the GKS-EDA scheme avoids the error of LMO-EDA which comes from the separated treatment of E_X and E_C functionals. The scheme can perform analysis both in the gas and in the condensed phases with most of the popular DFT functionals, including LDA, GGA, meta-GGA, hybrid GGA/meta-GGA, double hybrid, range-separated (long-range correction), and dispersion correction. By the GKS-EDA scheme, the DFT functionals assessment for hydrogen bonding, vdW interaction, symmetric radical cation, charge-transfer, and metal−ligand interaction is performed.

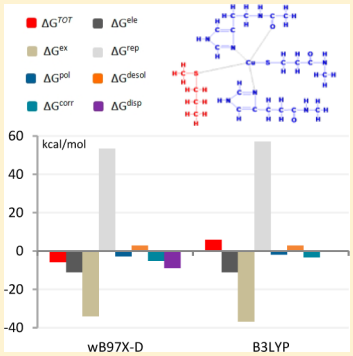

A. INTRODUCTION

As one of the useful tools for intermolecular interactions in quantum chemistry, the energy decomposition analysis (EDA) scheme divides the total interaction energy into several individual terms with ab initio molecular orbital (MO) theory or density functional theory (DFT) methods.[1−23] As one of the recently developed EDA schemes, the LMO-EDA (localized molecular orbital energy decomposition analysis) method provides analysis for open- or closed-shell interacting systems in the gas phase using Hartree−Fock (HF) orbitals or Kohn−Sham (KS) orbitals.[20] It divides the total HF or KS interaction energy ΔE^{TOT} into ΔE^{ele} (electrostatic), ΔE^{ex} (exchange), ΔE^{rep} (repulsion), ΔE^{pol} (polarization), and ΔE^{disp} (dispersion) terms. Due to its simplicity and robustness, the LMO-EDA scheme has been widely used for various weak and strong interactions.[24−40]

For the LMO-EDA analysis at the KS-DFT level, the exchange and dispersion terms are defined as the differences of the exchange (E_X) and correlation (E_C) functionals ongoing from monomers to supermolecule respectively. The repulsion and polarization terms are determined by KS orbitals and exchange functionals in certain intermediate steps. For most of DFT functionals, because the aim of the parametrization is to obtain accurate estimation of the total E_{XC}, the separated treatment of E_X and E_C in the LMO-EDA scheme would introduce the error into the individual interaction terms, leading to confused insight for some cases. For example, it is known that BLYP is not suitable for vdW interaction due to the lack of dispersion correction. However, for the T-shaped benzene dimer by BLYP, which will be discussed in the next section of this paper, the LMO-EDA analysis shows that the dispersion interaction plays the most important role for the vdW interaction. It does not make sense. Therefore, the analysis accuracy of LMO-EDA with DFT functional needs to be further improved. Moreover, the current LMO-EDA scheme cannot work with dispersion-corrected and range-separated functionals, resulting in the limited application of LMO-EDA. The functional adaptability of LMO-EDA need to be expanded.

One of the possible ways for improving the LMO-EDA scheme is to introduce the generalized Kohn−Sham (GKS) scheme proposed by Levy et al.[41] The GKS scheme maps a real system to an interacting model system represented by a single Slater determinant. In 2010, Baer et al. applied the GKS scheme to present systematic interpretations for range-separated and hybrid functionals, showing the accuracy of range-separated functionals for complicated electronic structure.[42]

The motivation of this work is to present a generalized Kohn−Sham based energy decomposition analysis scheme, named GKS-EDA, for interaction analysis in the gas and the condensed phase with various DFT functionals. Sequentially, GKS-EDA is employed in the assessment of various DFT functionals, which can be divided into five categories in this work.

The first category is local functional, involving local density approximation (LDA), generalized gradient approximation (GGA), and meta generalized gradient approximation (meta-GGA). The second category is a hybrid functional involving the exact HF exchange for functional description, including hybrid GGA and hybrid meta-GGA. The most popular hybrid GGA functional is B3LYP.[43,44] The hybrid meta-GGA functionals, for example, TPSSh,[45] M06-2X,[46] M08-HX,[47] etc., whose total energy depends on the occupied orbitals not only through the

Received: January 14, 2014
Revised: March 7, 2014
Published: March 10, 2014

HF exchange terms but also through the noninteracting spin kinetic energy densities, are shown to have better performance than local and hybrid GGA functionals.[47] The third category is double hybrid functional, which depends not only on occupied orbitals but also on unoccupied orbitals, for example, B2PLYP.[48] The fourth category is the dispersion-corrected functional, including vdW-DF,[49,50] DFT-D,[51−53] DCACP,[54] etc. DFT-D takes the dispersion effect into account with a damped dispersion correction, vdW-DF includes dispersion via nonlocal correlation in E_{XC} functional, whereas DCACP takes the form of pseudopotential for dispersion. The final category is range-separated functional, also called long-range correction functionals, including (1) the LC (LC: long-range correction) scheme by Hirao et al.,[55] (2) LC-ωPBE by Scuseria et al.,[56] (3) CAM-B3LYP by Handy et al.,[57] (4) the wB97 family (wB97, wB97X, and wB97X-D) by Head-Gordon et al.,[58,59] and (5) M11 by Truhlar et al.[60] These functionals focus on the correct asymptotic behavior of functionals by dividing the coulomb operator into two parts, one from the HF exact exchange for long-range and the other evaluated by DFT exchange functional for short range. In some range-separated functionals, such as wB97X,[58] small portion of the exact HF exchange is also involved in short-range exchange description. wB97X-D is a functional that combines range-separated treatment and dispersion correction.[59]

To guide DFT development for better performance, the GKS-EDA analysis with the DFT functionals mentioned above is employed for some typical interacting systems both in the gas phase and in the condensed phase, involving hydrogen bonding, vdW interaction, charge-transfer complex, open-shell cation, and metal−ligand interaction.

B. METHODOLOGY

1. GKS-EDA Scheme in the Gas Phase. In quantum mechanics, the ground-state energy is the minimum of the expectation value of the Hamiltonian with respect to many-electron wave function. The many-electron Hamiltonian $\hat{H}$ can be expressed as

$$\hat{H} = \hat{T} + \hat{V}_{ee} + \hat{V}_{ne} \tag{1}$$

$\hat{T}$ is the kinetic operator, $\hat{V}_{ee}$ is the electron−electron interaction operator, and $\hat{V}_{ne}$ is the nuclear-electron interaction operator, regarded as external potential operator.

According to the Hohenberg−Kohn theorem,[61] the total energy of a many-electron system is a unique functional of the electron density $\rho(r)$. The energy can be obtained by a variational principle. According to Levy, the minimum procedure can be written as[62,63]

$$E = \min_{\rho \to N} [\min_{\Psi \to \rho} [\langle \Psi | \hat{T} + \hat{V}_{ee} | \Psi \rangle] + \int \rho(r)\, v_{ne}(r)\, d^3r] \tag{2}$$

In eq 2, ρ and Ψ are the electronic density and wave function of an N-electron system, respectively. The inner minimum on the right-hand side of eq 2 can be defined as the universal HK (Hohenberg−Kohn) functional:

$$F(\rho) = \min_{\Psi \to \rho} \langle \Psi | \hat{T} + \hat{V}_{ee} | \Psi \rangle \tag{3}$$

In general, the HK functional is too complicated to solve. According to the Kohn−Sham scheme,[64,65] the calculation of Ψ can be replaced by a N-electron Slater determinant wave function Φ, which represents a noninteracting model system and gives the same ground-state density as Ψ. The expectation value of the Hamiltonian using the KS determinant Φ provides a large portion of the total energy whereas the remaining part is computed by the exchange−correlation functional, which is inherently local.

The nonlocal functionals, including hybrid, double hybrid, and range-separated types, are usually beyond the original Kohn−Sham framework because their exchange parts depend both on KS orbitals and density. They can be treated by the generalized Kohn−Sham (GKS) scheme.[41] In the GKS scheme, not only the noninteracting kinetic energy but also the part of electron−electron interaction is treated exactly. As denoted by Levy and Baer et al., the GKS form is flexible.[41,42] When the HK functional is defined as

$$F_S(\rho) = \min_{\Phi \to \rho} \langle \Phi | \hat{T} + \hat{V}_{ee} | \Phi \rangle \tag{4}$$

the GKS scheme is known as the Hartree−Fock−Kohn−Sham (HF-KS) scheme. By HF-KS, the correlation energy can be expressed as

$$E_C^{GKS} = F(\rho) - F_S(\rho) \tag{5}$$

ρ is achieved from the orbitals ϕ_i computed by the following equations:

$$\left(-\frac{1}{2}\nabla_i^2 + v_X^{GKS} + v_{ee} + v_{ne} + v_C^{GKS}\right)|\phi_i\rangle = \varepsilon_i |\phi_i\rangle \tag{6}$$

where

$$v_X^{GKS} = \frac{\delta E_X^{GKS}}{\delta \rho} \tag{7}$$

$$E_X^{GKS} = \langle \Phi^{GKS} | \hat{V}_{ee} | \Phi^{GKS} \rangle - J(\rho) \tag{8}$$

$$v_C^{GKS} = \frac{\delta E_C^{GKS}}{\delta \rho} \tag{9}$$

$$E_C^{GKS} = E_C(\rho) + (1 - \gamma)(E_X(\rho) - E_X^{GKS}) \tag{10}$$

In eq 8, $J(\rho)$ is the electron−electron repulsion energy. In eq 10, $E_X(\rho)$ and $E_C(\rho)$ are the exchange and correlation functionals, respectively. γ is the portion of the exact HF energy, ranging from 0 to 1.0. If double hybrid functional is applied, $E_C(\rho)$ is partially replaced by portion of MP2 correlation energy. In the KS scheme, the unknown energy is a density functional instead of an orbital functional, but in the GKS scheme, the exchange energy is exact, determined only by DFT orbitals, the electronic correlation energy is accounted for by E_C^{GKS}, determined by density and orbitals simultaneously. As claimed by Baer et al., "E_C^{GKS} encapsulates the entire immensity of the electronic structure problem, and it is this functional for which approximation must be crafted under DFT".[42]

The parentheses in the left-hand side of eq 6 can be written as

$$\hat{F}^{GKS} = \hat{F}^{D} + v_C^{GKS} \tag{11}$$

$$\hat{F}^{D} = -\frac{1}{2}\nabla^2 + v_X^{GKS} + v_{ee} + v_{ne} \tag{12}$$

For a supermolecule consisting of monomers, the total interaction energy ΔE^{TOT} is expressed as

dx.doi.org/10.1021/jp500405s | J. Phys. Chem. A 2014, 118, 2531−2542

$$\Delta E^{\mathrm{TOT}} = \langle\Phi_{\mathrm{S}}|\hat{F}_{\mathrm{S}}^{\mathrm{GKS}}|\Phi_{\mathrm{S}}\rangle - \sum_{\mathrm{M}}\langle\Phi_{\mathrm{M}}|\hat{F}_{\mathrm{M}}^{\mathrm{GKS}}|\Phi_{\mathrm{M}}\rangle$$
$$= (\langle\Phi_{\mathrm{S}}|\hat{F}_{\mathrm{S}}^{\mathrm{D}}|\Phi_{\mathrm{S}}\rangle - \sum_{\mathrm{M}}\langle\Phi_{\mathrm{M}}|\hat{F}_{\mathrm{M}}^{\mathrm{D}}|\Phi_{\mathrm{M}}\rangle)$$
$$+ (\langle\Phi_{\mathrm{S}}|v_{\mathrm{C}}^{\mathrm{GKS}}(\mathrm{S})|\Phi_{\mathrm{S}}\rangle - \sum_{\mathrm{M}}\langle\Phi_{\mathrm{M}}|v_{\mathrm{C}}^{\mathrm{GKS}}(\mathrm{M})|\Phi_{\mathrm{M}}\rangle) \quad (13)$$

S and M denote supermolecule and monomer, respectively. Followed by the previous EDA schemes such as the Kitaura−Morokuma scheme and all the related variants,[1−4,20,66,67] the first bracket in the right-hand side of eq 13 can be decomposed into the electrostatic, exchange, repulsion, and polarization terms:

$$\langle\Phi_{\mathrm{S}}|\hat{F}_{\mathrm{S}}^{\mathrm{D}}|\Phi_{\mathrm{S}}\rangle - \sum_{\mathrm{M}}\langle\Phi_{\mathrm{M}}|\hat{F}_{\mathrm{M}}^{\mathrm{D}}|\Phi_{\mathrm{M}}\rangle$$
$$= \Delta E^{\mathrm{ele}} + \Delta E^{\mathrm{ex}} + \Delta E^{\mathrm{rep}} + \Delta E^{\mathrm{pol}} \quad (14)$$

These interaction terms can be obtained gradually by several intermediate states. In step 0, there is not any interaction among monomers. The wave function of step 0, Φ^{DP}, is the product of monomers' wave function:

$$\Phi^{\mathrm{DP}} = \prod_{\mathrm{M}}\Phi_{\mathrm{M}} \quad (15)$$

When the counterpoise (CP) method is applied for the basis set superposition error (BSSE), the Kohn−Sham orbitals in Φ_{M} are expanded with supermolecule's basis set.[68]

The energy of the step 0 can be expressed as

$$E_{\mathrm{S}}^{(0)} = \langle\Phi^{\mathrm{DP}}|\sum_{\mathrm{M}}\hat{F}_{\mathrm{M}}^{\mathrm{D}}|\Phi^{\mathrm{DP}}\rangle$$
$$= \sum_{\mathrm{M}}\langle\Phi_{\mathrm{M}}|\hat{F}_{\mathrm{M}}^{\mathrm{D}}|\Phi_{\mathrm{M}}\rangle \quad (16)$$

At step 1, there is not any orbital overlap among monomers. The wave function Φ^{DP} is unchanged. If the sum of monomers' GKS operators $\hat{F}_{\mathrm{M}}^{\mathrm{D}}$ is replaced by the supermolecule's GKS operator $\hat{F}_{\mathrm{S}}^{\mathrm{D}}$, the corresponding energy $E_{\mathrm{S}}^{(1)}$ can be written as

$$E_{\mathrm{S}}^{(1)} = \langle\Phi^{\mathrm{DP}}|\hat{F}_{\mathrm{S}}^{\mathrm{D}}|\Phi^{\mathrm{DP}}\rangle \quad (17)$$

From the step 0 to the step 1, the electrostatic interaction arising from the variation of the GKS operators with the wave function Φ^{DP}, can be defined as

$$\Delta E^{\mathrm{ele}} = \langle\Phi^{\mathrm{DP}}|\hat{F}_{\mathrm{S}}^{\mathrm{D}}|\Phi^{\mathrm{DP}}\rangle - \sum_{\mathrm{M}}\langle\Phi_{\mathrm{M}}|\hat{F}_{\mathrm{M}}^{\mathrm{D}}|\Phi_{\mathrm{M}}\rangle \quad (18)$$

For the step 2, the orbital overlap among monomers is taken into considered. The wave function must be in the antisymmetric and normalized form:

$$\Phi^{\mathrm{ASN}} = \hat{A}\Phi^{\mathrm{DP}} \quad (19)$$

In eq 19, $\hat{A}$ is the antisymmetrization operator. With the requirement for antisymmetry and orthonormality of DFT orbitals, the corresponding approximate energy $E_{\mathrm{S}}^{(2)}$ can be expressed as

$$E_{\mathrm{S}}^{(2)} = \langle\Phi^{\mathrm{ASN}}|\hat{F}_{\mathrm{S}}^{\mathrm{D}}|\Phi^{\mathrm{ASN}}\rangle \quad (20)$$

The electronic density from the antisymmetrized and normalized wave function Φ^{ASN}, compared to that from Φ^{DP}, decreases between monomers and increases at the side of each monomer remote from the other, leading to repulsive force among monomers.[67] The energy difference between steps 1 and 2 is defined as exchange repulsion interaction:

$$\Delta E^{\mathrm{exrep}} = \langle\Phi^{\mathrm{ASN}}|\hat{F}_{\mathrm{S}}^{\mathrm{D}}|\Phi^{\mathrm{ASN}}\rangle - \langle\Phi^{\mathrm{DP}}|\hat{F}_{\mathrm{S}}^{\mathrm{D}}|\Phi^{\mathrm{DP}}\rangle \quad (21)$$

As proposed by Stone and Li et al.,[20,66,67] the $\Delta E^{\mathrm{exrep}}$ can be further divided into the exchange term ΔE^{ex} and the repulsion term ΔE^{rep}. The exchange term ΔE^{ex} is explicitly expressed as the variation of the GKS exchange energy $E_{\mathrm{X}}^{\mathrm{GKS}}$ from step 1 to step 2.

$$\Delta E^{\mathrm{ex}} = E_{\mathrm{X}}^{\mathrm{GKS}}(2) - E_{\mathrm{X}}^{\mathrm{GKS}}(1) \quad (22)$$

The repulsion energy is then defined as

$$\Delta E^{\mathrm{rep}} = \Delta E^{\mathrm{exrep}} - \Delta E^{\mathrm{ex}} \quad (23)$$

At step 3, with the SCF procedure, Φ^{ASN} is optimized as Φ_{S}. The polarization energy can be defined as

$$\Delta E^{\mathrm{pol}} = \langle\Phi_{\mathrm{S}}|\hat{F}_{\mathrm{S}}^{\mathrm{D}}|\Phi_{\mathrm{S}}\rangle - \langle\Phi^{\mathrm{ASN}}|\hat{F}_{\mathrm{S}}^{\mathrm{D}}|\Phi^{\mathrm{ASN}}\rangle \quad (24)$$

Equation 24 means that the polarization term is equal to orbital relaxation energy by the SCF procedure. In some EDA schemes, orbital relaxation energy includes polarization and charge transfer. However, as said by Davidson et al.: "This partitioning is not clean because it depends on grouping the basis set into functions associated with each monomer .... In the limit of a complete basis set on both A and B, the charge transfer and polarization in these definitions become equivalent."[69] In GKS-EDA, it is preferred that only polarization energy is used since monomers' orbitals are expanded using supermolecule's basis set for BSSE correction.

The second bracket in the right-hand side of eq 13, illustrating the difference of the GKS correlation energy from monomers to supermolecule, can be defined as the correlation term:

$$\Delta E^{\mathrm{corr}} = \langle\Phi_{\mathrm{S}}|v_{\mathrm{C}}^{\mathrm{GKS}}(\mathrm{S})|\Phi_{\mathrm{S}}\rangle - \sum_{\mathrm{M}}\langle\Phi_{\mathrm{M}}|v_{\mathrm{C}}^{\mathrm{GKS}}(\mathrm{M})|\Phi_{\mathrm{M}}\rangle \quad (25)$$

Using eq 10, the correlation term can be further written as

$$\Delta E^{\mathrm{corr}} = \Delta E_{\mathrm{C}}(\rho) + (1-\gamma)(\Delta E_{\mathrm{X}}(\rho) - \Delta E_{\mathrm{X}}^{\mathrm{GKS}}) \quad (26)$$

where $\Delta E_{\mathrm{C}}(\rho)$ and $\Delta E_{\mathrm{X}}(\rho)$ are the difference of the exchange and correlation functionals between monomers and supermolecule.

If double hybrid functional is applied, ΔE^{corr} can be expressed as

$$\Delta E^{\mathrm{corr}} = (1-\gamma)\cdot(\Delta E_{\mathrm{X}} - \Delta E_{\mathrm{X}}^{\mathrm{GKS}}) + (1-C_{\mathrm{MP2}})\cdot\Delta E_{\mathrm{C}}$$
$$+ C_{\mathrm{MP2}}\cdot\Delta E_{\mathrm{MP2}}^{(2)} \quad (27)$$

where $\Delta E_{\mathrm{MP2}}^{(2)}$ is the MP2 correlation energy from DFT orbitals with the amount accounted by C_{MP2}.

Specifically, when dispersion corrected DFT is applied, an extra term ΔE^{disp} accounting the dispersion interaction is introduced:

$$\Delta E^{\mathrm{disp}} = E_{\mathrm{S}}^{\mathrm{disp}} - \sum_{\mathrm{M}}E_{\mathrm{M}}^{\mathrm{disp}} \quad (28)$$

If Grimme's DFT-D scheme is specified, the E^{disp} can be expressed as[51−53]

dx.doi.org/10.1021/jp500405s | J. Phys. Chem. A 2014, 118, 2531−2542

$$E^{\mathrm{disp}} = -\sum_{\mathrm{AB}}\sum_{n=6,8,10} s_n \frac{C_n^{\mathrm{AB}}}{R_{\mathrm{AB}}^n} f_{\mathrm{damp}}(R_{\mathrm{AB}}) \tag{29}$$

In eq 29 the summation is over all atom pairs in the supermolecule, s_n are global (functional dependent) scaling factors, C_n^{AB} is the averaged nth dispersion coefficient for atom pair AB, R_{AB} is the distance between atoms A and B, and f_{damp} are damping functions determining the range of the dispersion correction.

In summary, for the gas phase, the GKS-EDA scheme divides the total interaction energy into the following terms with the final term optional for DFT-D:

$$\Delta E^{\mathrm{TOT}} = \Delta E^{\mathrm{ele}} + \Delta E^{\mathrm{ex}} + \Delta E^{\mathrm{rep}} + \Delta E^{\mathrm{pol}} + \Delta E^{\mathrm{corr}} + \Delta E^{\mathrm{disp}} \tag{30}$$

It is worthwhile to point out the difference between LMO-EDA and GKS-EDA here. In LMO-EDA, the contribution of E_{XC} functionals is divided into E_{X} and E_{C}, which uniquely determine the ΔE^{ex} and ΔE^{disp} terms, respectively. The ΔE^{rep} and ΔE^{pol} terms are determined by the KS orbitals and E_{X} functional together. In GKS-EDA, the contribution of the E_{XC} functional is not separated. The ΔE^{corr} is defined as the GKS correlation energy from monomers to supermolecule, while the other terms are governed by DFT orbitals.

2. GKS-EDA Scheme in Solution. Intermolecular interactions in various solvated environments are significant, which can be well understood by condensed phase energy decomposition analysis schemes by Tomasi,[70] de1 Valle,[71] Robert,[72] Bickelhaupt,[73] Fedorov,[74] and Su[75] etc. EDA-PCM is proposed by our group on the basis of LMO-EDA and implicit solvation model PCM. In EDA-PCM,[75] solvent molecules are considered as dielectric medium and polarized by the charge distribution of solute molecule. The solute molecule is inserted into a cavity (or cavities) in the dielectric medium. The interaction between the solute charges and the polarized electric field of the solvent is represented as a reaction field operator and then put into self-consistent reaction field (SCRF) procedure.[56,76,77] Various kinds of the PCM methods, including CPCM,[78,79] IEFPCM[80−83] and HET-CPCM,[84] can be employed in EDA-PCM.

In this part, GKS-EDA is extended to the condensed phase based on the framework of EDA-PCM.[75] In general, the total solvation free energy in solution can be expressed as

$$\Delta G^{\mathrm{SOL}} = \Delta G^{\mathrm{ele}} + \Delta G^{\mathrm{non-ele}} + \Delta G^{\mathrm{cav}} \tag{31}$$

ΔG^{cav} is the free energy cost for creating cavities of solute molecules in solvated environment characterized by single dielectric continuum. $\Delta G^{\mathrm{nonele}}$ is the nonelectronic free energy, including dispersion, repulsion, and vdW interaction between solvent and solute molecules. ΔG^{ele}, the electronic free energy determined by the solute molecule's wave function, is the most important according to the theoretical hypothesis of implicit solvation models. In this paper, only ΔG^{ele} is taken into account for the influence of solvent environment to the intermolecular interaction.

On the basis of the DFT descriptions of PCM,[77] the density in the condense phase ρ^{SOL} is achieved from the orbitals ϕ_i^{SOL} computed by the following equations:

$$(F^{\mathrm{GKS}} + v^{\mathrm{SOL}})|\phi_i^{\mathrm{SOL}}\rangle = \varepsilon_i^{\mathrm{SOL}}|\phi_i^{\mathrm{SOL}}\rangle \tag{32}$$

In eq 32, v^{SOL} is the reaction field operator, determined by the PCM methodology (CPCM, IEFPCM, and HET-PCM in this paper) and the cavity tesserae scheme. In EDA-PCM and GKS-EDA, the monomers' cavities are constructed by the fixed points with the variable areas (FIXPVA) scheme proposed by Su and Li,[85] which ensures that the total interaction energy and individual EDA terms change smoothly along with the whole potential energy surface.

The solute's total free energy can be expressed as

$$G^{\mathrm{TOT}} = \langle \Phi^{\mathrm{SOL}}|F^{\mathrm{GKS}}|\Phi^{\mathrm{SOL}}\rangle + \Delta G^{\mathrm{SOL}} \tag{33}$$

In eq 33, Φ^{SOL} is the solute's wave function. ΔG^{SOL} denotes the free energy arising from solvent−solute electronic interactions, determined by reaction field operator and solute's wave function.

Considering a supermolecule S formed by a number of monomers M immersed in a polarizable medium, the total interaction free energy ΔG^{TOT} is expressed as

$$\begin{aligned}\Delta G^{\mathrm{TOT}} &= G_{\mathrm{S}}^{\mathrm{TOT}} - \sum_{\mathrm{M}} G_{\mathrm{M}}^{\mathrm{TOT}} \\ &= (\langle \Phi_{\mathrm{S}}^{\mathrm{SOL}}|F_{\mathrm{S}}^{\mathrm{GKS}}|\Phi_{\mathrm{S}}^{\mathrm{SOL}}\rangle - \sum_{\mathrm{M}} \langle \Phi_{\mathrm{M}}^{\mathrm{SOL}}|F_{\mathrm{M}}^{\mathrm{GKS}}|\Phi_{\mathrm{M}}^{\mathrm{SOL}}\rangle) \\ &\quad + (\Delta G_{\mathrm{S}}^{\mathrm{SOL}} - \sum_{\mathrm{M}} \Delta G_{\mathrm{M}}^{\mathrm{SOL}})\end{aligned} \tag{34}$$

The first parentheses in the right-hand side of eq 34, describing the variation of the solvation free energy by KS determinant from monomers to supermolecule, can be further decomposed into electrostatic, exchange, repulsion, polarization, and correlation terms:

$$\begin{aligned}&\langle \Phi_{\mathrm{S}}^{\mathrm{SOL}}|F_{\mathrm{S}}^{\mathrm{GKS}}|\Phi_{\mathrm{S}}^{\mathrm{SOL}}\rangle - \sum_{\mathrm{M}} \langle \Phi_{\mathrm{M}}^{\mathrm{SOL}}|F_{\mathrm{M}}^{\mathrm{GKS}}|\Phi_{\mathrm{M}}^{\mathrm{SOL}}\rangle \\ &\quad = \Delta G^{\mathrm{ele}} + \Delta G^{\mathrm{ex}} + \Delta G^{\mathrm{rep}} + \Delta G^{\mathrm{pol}} + \Delta G^{\mathrm{corr}}\end{aligned} \tag{35}$$

The expressions of ΔG^{ele}, ΔG^{ex}, ΔG^{rep}, ΔG^{pol}, and ΔG^{corr} are the same with ΔE^{ele}, ΔE^{ex}, ΔE^{rep}, ΔE^{pol}, and ΔE^{corr}, respectively. The notation "G" is applied instead of "E" because these interaction terms are determined by Φ^{SOL} and ρ^{SOL} in the condensed phase instead of Φ and ρ in the gas phase.

The second parentheses in the right-hand side of eq 34, which accounts the free energy penalty by environment due to monomers' interaction, defined as the desolvation term $\Delta G^{\mathrm{desol}}$:

$$\Delta G^{\mathrm{desol}} = \Delta G_{\mathrm{S}}^{\mathrm{SOL}} - \sum_{\mathrm{M}} \Delta G_{\mathrm{M}}^{\mathrm{SOL}} \tag{36}$$

Finally, if dispersion correction DFT is applied, the dispersion term ΔG^{disp} is introduced. When the Grimme's correction DFT is specified, the ΔG^{disp} definition is same with the ΔE^{disp} one.

In summary, the total interaction energy in the condensed phase is decomposed into electrostatic, exchange, repulsion, polarization, correlation, and dispersion terms:

$$\Delta G^{\mathrm{TOT}} = \Delta G^{\mathrm{ele}} + \Delta G^{\mathrm{ex}} + \Delta G^{\mathrm{rep}} + \Delta G^{\mathrm{pol}} + \Delta G^{\mathrm{desol}} + \Delta G^{\mathrm{corr}} + \Delta G^{\mathrm{disp}} \tag{37}$$

C. COMPUTATIONAL DETAILS

All calculations were performed with the quantum chemistry program package GAMESS.[86] Based on LMO-EDA, the GKS-EDA scheme is implemented, which may be available in the released version of GAMESS recently. The counterpoise (CP) method is applied for basis set superposition error (BSSE) without dispersion correction.[68]

dx.doi.org/10.1021/jp500405s | J. Phys. Chem. A 2014, 118, 2531−2542

As for the test examples in the gas phase, the four complexes shown in Figure 1 are selected, including the water dimer,

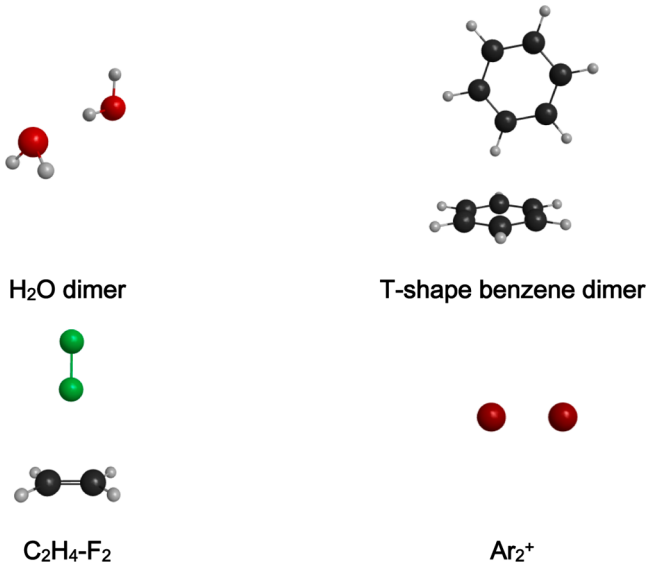

Figure 1. Geometries of the water dimer, benzene dimer, $C_2H_4\cdots F_2$ and Ar_2^+ complexes.

benzene dimer, $C_2H_4\cdots F_2$, and Ar_2^+. The aug-cc-pVnZ (n = D, T) and cc-pVTZ basis sets were employed, denoted as ACCD, ACCT, and CCT, respectively, in the following discussions. The geometries of the water dimer, $C_2H_4\cdots F_2$, and Ar_2^+ are optimized at the MP2/ACCT level, and the benzene dimer is optimized at the MP2/ACCD level.

As for the test example in the condense phase, the copper ligand model molecule for the active site of the type 1 copper protein is chosen.[87] The 6-31G(d) basis set was used. The CPCM method[78,79] with the UFF radii model scaled by a factor of 1.1 is employed.[88] The dielectric constant ϵ is set as 20.0 for the protein environment.

The functionals tested in this work involved the LDA, GGA, meta-GGA, hybrid GGA/meta-GGA, double hybrid, range-separated (long-range correction), and dispersion correction types. They are shown in Table 1, including BLYP,[89,90] B3LYP,[43,44] LC-BLYP,[55] CAM-B3LYP,[57] B2PLYP,[48] BLYP-D,[51] B97,[91] B97-D,[92] wB97,[58] wB97X,[58] wB97X-D,[59] M06-L,[93] M06-2X,[46] and M11.[60] For the water dimer, $C_2H_4\cdots F_2$ and Ar_2^+ complexes, all the DFT functionals in Table 1 are employed. For the benzene dimer and the copper ligand model molecule, only some of them are used for brief.

D. RESULTS AND DISCUSSIONS

1. Water Dimer. Table 2 shows the GKS-EDA analysis results with the ACCT basis set for the water dimer interaction. The best theoretical estimated interaction energy is ∼−5.02 kcal/mol at the CCSD(T)/complete basis set (CBS) level,[94,95] whereas the corresponding experimental value is −5.40 kcal/mol.[96]

By the GKS-EDA analysis, as a typical hydrogen bond, besides the electrostatic interaction, the water dimer interaction also includes the obvious correlation and dispersion contributions. The ΔE^{disp} term only exists in the analysis by B97-D, BLYP-D, and wB97X-D functionals. First, the BLYP, B3LYP, and B97 functionals underestimate the total interaction energies because of the small correlation terms. As a double hybrid functional, B2PLYP slightly enhances the description of the total binding energy compared to BLYP and B3LYP due to the small repulsive term. The meta-GGA functional M06-L provides the smallest ΔE^{ele}, ΔE^{ex}, and ΔE^{rep} among all the test functionals, leading to the moderate total binding energy of −4.61 kcal/mol. Owing to the larger ΔE^{ele} and ΔE^{corr} terms, M06-2X's total interaction energy is better than M06-L.

Second, the range-separated DFT functionals, except M11, tend to mimic the dispersion interaction by relatively large correlation energy, in agreement with the comment by Ziegler and Grimme et al.[97] As a result of the appropriate description for the correlation interaction, CAM-B3LYP is able to predict the hydrogen bonding quite well, whereas, because of the quite large correlation terms, LC-BLYP, wB97, and wB97X somewhat overestimate the total interaction energies. The total interaction energy by M11 is the smallest among all the tested range-separated functionals due to the small correlation term.

Third, in the GKS-EDA analysis by B97-D, BLYP-D, and wB97X-D, there are two significant terms for the hydrogen bonding, including ΔE^{corr} and ΔE^{disp}. B97-D and BLYP-D provide the similar ΔE^{disp} values. Their performance is attributed to the ΔE^{corr} terms, leading to the total energies of −4.92 and −4.30 kcal/mol by BLYP-D and B97-D, respectively. By wB97X-D, given the additional dispersion term, the ΔE^{corr} value is relatively small to avoid the overestimation, leading to a satisfied total interaction energy.

2. Benzene Dimer. Table 3 shows the GKS-EDA analysis results for the T-shaped benzene dimer using the CCD, CCT, and ACCT basis sets by B97-D, BLYP-D, wB97X-D, LC-BLYP, M06-2X, and B2PLYP. The GKS-EDA analysis shows that the performance is controlled by the dispersion and correlation terms. The other interaction terms by the different functionals are similar.

First, the dispersion correction DFT functionals predict the binding energies quite well, close to the estimated CCSD(T)/CBS value of −2.84 kcal/mol by Kim et al.[95] With the variation of the basis sets, their total interaction energies along with the

Table 1. DFT Functionals Used in This Work

type	functional name
GGA	BLYP
hybrid GGA	B3LYP, B97
meta-GGA	M06-L
hybrid meta-GGA	M06-2X
range-separated	LC-BLYP, CAM-B3LYP, M11, wB97, wB97X
dispersion correction, GGA	BLYP-D, B97-D
range-separated + dispersion corrections	wB97X-D

dx.doi.org/10.1021/jp500405s | J. Phys. Chem. A 2014, 118, 2531−2542

Table 2. GKS-EDA Analysis for the Water Dimer with the ACCT Basis Set (kcal/mol)

	ΔE^{ele}	ΔE^{ex}	ΔE^{rep}	ΔE^{pol}	ΔE^{corr}	ΔE^{disp}	ΔE^{TOT}
BLYP	−8.34	−11.65	20.00	−2.82	−1.21		−4.03
B3LYP	−8.32	−10.77	18.79	−2.84	−1.35		−4.49
LC-BLYP	−8.74	−11.55	19.68	−2.45	−3.54		−6.59
CAM-B3LYP	−8.47	−10.77	18.73	−2.74	−1.99		−5.23
B2PLYP	−8.35	−9.90	17.55	−2.77	−1.25		−4.72
BLYP-D	−8.34	−11.65	20.00	−2.82	−1.21	−0.89	−4.92
M06-L	−7.76	−9.12	16.50	−2.90	−1.32		−4.61
M06-2X	−8.27	−9.83	17.36	−2.64	−1.75		−5.12
M11	−8.30	−9.80	17.41	−2.69	−1.30		−4.68
B97	−8.16	−10.37	18.24	−2.87	−1.27		−4.41
wB97	−8.26	−10.24	17.92	−2.44	−2.66		−5.69
wB97X	−8.22	−10.06	17.74	−2.54	−2.56		−5.63
wB97X-D	−8.13	−9.82	17.52	−2.72	−1.35	−0.47	−4.97
B97-D	−8.08	−10.67	18.78	−2.91	−0.49	−0.94	−4.30

Table 3. GKS-EDA Analysis for the T-Shaped Benzene Dimer with the CCD, CCT, and ACCT Basis Sets (kcal/mol)

method	basis set	ΔE^{ele}	ΔE^{ex}	ΔE^{rep}	ΔE^{pol}	ΔE^{corr}	ΔE^{disp}	ΔE^{TOT}
B97-D	ACCT	−3.36	−13.62	22.76	−1.66	−0.34	−6.23	−2.46
	CCT	−3.40	−13.66	22.76	−1.65	−0.29	−6.23	−2.47
	CCD	−3.53	−13.80	22.86	−1.53	−0.23	−6.23	−2.46
BLYP-D	ACCT	−3.59	−14.74	24.25	−1.78	−0.61	−5.63	−2.10
	CCT	−3.65	−14.80	24.28	−1.77	−0.58	−5.63	−2.14
	CCD	−3.78	−14.90	24.32	−1.57	−0.62	−5.63	−2.17
wB97X-D	ACCT	−3.29	−13.01	21.73	−1.64	−2.86	−3.36	−2.43
	CCT	−3.32	−13.03	21.72	−1.63	−2.81	−3.36	−2.44
	CCD	−3.44	−13.20	21.84	−1.58	−2.67	−3.36	−2.41
LC-BLYP	ACCT	−3.81	−15.14	24.40	−1.58	−5.17		−1.30
	CCT	−3.86	−15.17	24.40	−1.55	−5.14		−1.33
	CCD	−3.94	−15.23	24.39	−1.64	−4.78		−1.19
M06-2X	ACCT	−3.46	−13.43	22.12	−1.37	−5.95		−2.09
	CCT	−3.48	−13.46	22.12	−1.39	−5.84		−2.04
	CCD	−3.58	−13.51	22.15	−1.56	−5.51		−2.00
B2PLYP	ACCT	−3.49	−13.88	22.75	−1.61	−3.57		0.22
	CCT	−3.53	−13.90	22.75	−1.58	−3.34		0.38
	CCD	−3.64	−13.96	22.74	−1.48	−2.75		0.92

Table 4. LMO-EDA and GKS-EDA Analysis by BLYP for the T-Shaped Benzene Dimer with the CCD, CCT and ACCT Basis Sets (kcal/mol)

	basis set	ΔE^{ele}	ΔE^{ex}	ΔE^{rep}	ΔE^{pol}	ΔE^{corr}	ΔE^{disp}	ΔE^{TOT}
GKS-EDA	ACCT	−3.59	−14.74	24.25	−1.78	−0.61		3.53
	CCT	−3.65	−14.80	24.28	−1.77	−0.58		3.48
	CCD	−3.78	−14.90	24.32	−1.57	−0.62		3.46
LMO-EDA	ACCT	−3.59	−0.45	13.69	−1.84		−4.28	3.53
	CCT	−3.65	−0.51	13.70	−1.79		−4.27	3.48
	CCD	−3.78	−0.69	13.74	−1.62		−4.18	3.46

individual interaction terms remain stable. The total interaction energies are governed by the dispersion terms, which are −6.23, −5.63, and −3.36 kcal/mol by B97-D, BLYP-D, and wB97X-D, respectively, with the ACCT basis set. For wB97X-D, the small dispersion value is compensated by the large correlation term, leading to the proper total interaction energy.

Second, similar to the analysis for the water dimer, LC-BLYP and M06-2X provide extra correlation terms to mimic the dispersion interaction, leading to the attractive binding energies. In detail, with the ACCT basis set, the correlation values of LC-BLYP and M06-2X, −5.17 and −5.95 kcal/mol respectively, are close to the sum of ΔE^{corr} and ΔE^{disp} in the analysis results by B97-D, BLYP-D, and wB97X-D. With the larger correlation value, the performance of M06-2X is better than that of LC-BLYP.

Third, as for B2PLYP, the performance is more sensitive to the basis set variations. Although the MP2 correlation energy is involved in the correlation term, the ΔE^{corr} values, −2.75, −3.34, and −3.57 kcal/mol using CCD, CCT, and ACCT, respectively, are smaller than those by M06-2X and LC-BLYP, leading to the repulsive total interaction energy.

Finally, to explore the error of LMO-EDA mentioned in the Introduction, the LMO-EDA and GKS-EDA analysis results for the T-shaped benzene dimer by the BLYP functional are listed in Table 4. By the two EDA schemes, it is shown that BLYP provides the repulsive description for the benzene interaction.

dx.doi.org/10.1021/jp500405s | J. Phys. Chem. A 2014, 118, 2531−2542

Table 5. GKS-EDA Analysis for $C_2H_4\cdots F_2$ with the ACCT Basis Set (kcal/mol)

	ΔE^{ele}	ΔE^{ex}	ΔE^{rep}	ΔE^{pol}	ΔE^{corr}	ΔE^{disp}	ΔE^{TOT}
BLYP	−3.02	−7.46	13.59	6.32	−12.19		−2.76
B3LYP	−2.98	−7.30	13.41	1.68	−6.29		−1.47
B2PLYP	−3.06	−7.41	13.67	−1.00	−3.37		−1.18
LC-BLYP	−3.15	−7.75	13.88	−0.31	−5.02		−2.35
CAM-B3LYP	−3.03	−7.41	13.53	−0.27	−4.05		−1.22
M06-L	−2.32	−5.47	10.55	3.67	−8.77		−2.35
M06-2X	−2.82	−6.89	12.73	−0.76	−3.67		−1.40
M11	−2.64	−6.61	12.21	−1.03	−2.47		−0.54
B97	−2.88	−6.98	12.93	1.51	−6.06		−1.48
wB97	−2.86	−6.94	12.71	−0.64	−3.59		−1.31
wB97X	−2.89	−6.92	12.82	−0.63	−3.55		−1.18
wB97X-D	−2.82	−6.72	12.59	−0.36	−2.81	−0.62	−0.75
BLYP-D	−3.02	−7.46	13.59	6.32	−12.19	−1.20	−3.96
B97-D	−2.82	−6.83	12.74	6.11	−11.14	−1.44	−3.37

As for GKS-EDA, the positive total interaction by BLYP arises from the lack of the dispersion interaction and the relatively small correlation term. However, as illustrated by LMO-EDA, the dispersion interaction is the largest contribution ranging from −4.18 to −4.28 kcal/mol with the various basis sets, even larger than the ΔE^{ele} value. The LMO-EDA result contradicts our knowledge of the vdW interaction, whereas the GKS-EDA analysis is physical meaningful.

3. $C_2H_4\cdots F_2$ Complex. Table 5 shows the GKS-EDA analysis for the $C_2H_4\cdots F_2$ complex with the ACCT basis set. The ethylene−halogen complex is important for the mechanism of the addition reaction of halogen molecule to ethylene. One of the theoretical viewpoints considers the charge transfer from the π orbital of C_2H_4 toward the halogen molecule as the main contribution of the stabilization energy,[98] whereas another viewpoint is that the dispersion interaction is more important than the charge transfer effect.[99] As illustrated by Chai et al., most of DFT functionals tend to overestimate the binding energy.[58]

The GKS-EDA analysis illustrates that the DFT performance is mainly attributed to the polarization and correlation terms. The total binding energies vary from −0.54 to −3.46 kcal/mol, compared to the best estimated value of −1.07 kcal/mol by Truhlar et al.[100] First, the local functionals, involving BLYP, BLYP-D, M06-L, and B97-D, overestimate the total interaction energy along with the large correlation and the positive polarization terms. By BLYP, the ΔE^{corr} is −12.19 kcal/mol whereas the ΔE^{pol} is 6.32 kcal/mol, showing that the polarization energy is a repulsive effect. BLYP-D and B97-D give even larger total interaction energies compared to BLYP and B97, respectively, because of the additional dispersion term. As for the hybrid functionals B97 and B3LYP, the analysis results show the proper total interaction energies with the positive ΔE^{pol} and large ΔE^{corr} values.

Second, for all the range-separated DFT functionals along with M06-2X and B2PLYP, their analysis results are similar, showing the small negative ΔE^{pol} and the relatively small ΔE^{corr} values. The polarization interaction is not important, the total interaction is governed by the correlation term, regarded as the typical vdW interaction. For example, the wB97X interaction energy is −1.18 kcal/mol, with ΔE^{ele} = −2.64 kcal/mol, ΔE^{ex} = −6.92 kcal/mol, ΔE^{rep} = 12.82 kcal/mol, ΔE^{pol} = −0.63 kcal/mol, and ΔE^{corr} = −3.55 kcal/mol. All these functionals except LC-BLYP aviod the overstimation of the binding energy. Arising from the large correlation value, LC-BLYP overpredicts the interaction energy. As concluded by Corminboeuf et al.,[34] the large portion of the exact HF exchange energy is helpful to improve the interaction description for the ethylene-halogen complex.

Finally, the behavior of the GKS-EDA polarization interaction can be examined by the electron density difference map (EDDM), which is defined as the difference between the electron density maps of monomers and that of supermolecule. The EDDMs of BLYP, B3LYP, LC-BLYP, and B2PLYP for the $C_2H_4\cdots F_2$ and the water dimer are shown in Table 6, in which

Table 6. Electron Density Difference Maps (EDDMs) of the Water Dimer and $C_2H_4\cdots F_2$ with the ACCT Basis Set[a]

DFT	water dimer	C_2H_4-F_2
B2PLYP	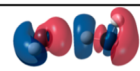	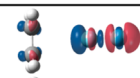
M06-2X		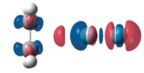
CAM-B3LYP	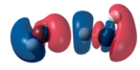	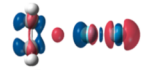
B3LYP		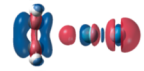
BLYP		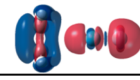

[a]The red and blue parts in the EDDMs denote the increase and decrease of the electron density arising from the interaction, respectively.

the red and blue parts denote the increase and decrease of the electron density arising from the interaction, respectively. For the water dimer, it is shown that the EDDMs from the vairous DFT functionals are similar, according to the fact that their polarization values are close. As for the $C_2H_4\cdots F_2$ complex, the EDDMs are quite different. The EDDM by BLYP shows the extinct electron transfer from the π orbital of C_2H_4 to the σ_u* orbital of F_2. It leads to the instability of the energy by the SCF procedure and the positive polarization interaction, which can be compensated by the large correlation energy. The EDDM of B3LYP is analogous to the BLYP one, compared to the similarity of their positive polarization terms, whereas for the functionals providing small negative polarization values, their EDDMs show that the electron density of the F atom that is

dx.doi.org/10.1021/jp500405s | J. Phys. Chem. A 2014, 118, 2531−2542

Table 7. GKS-EDA Analysis for Ar_2^+ with the ACCT Basis Set (kcal/mol)

	ΔE^{ele}	ΔE^{ex}	ΔE^{rep}	ΔE^{pol}	ΔE^{corr}	ΔE^{disp}	ΔE^{TOT}
BLYP	−9.68	−31.03	67.95	−38.71	−35.38		−46.85
B3LYP	−9.26	−30.07	66.10	−39.40	−29.43		−42.06
B2PLYP	−8.94	−29.31	64.54	−40.30	−22.89		−36.90
LC-BLYP	−9.88	−31.73	68.78	−40.75	−29.80		−43.39
CAM-B3LYP	−9.35	−30.85	66.48	−40.20	−26.23		−39.66
BLYP-D	−9.68	−31.03	67.95	−38.71	−35.38	−0.12	−46.97
M06-L	−7.25	−25.58	57.78	−35.65	−33.18		−43.88
M06-2X	−8.84	−29.34	64.43	−39.98	−24.11		−37.84
M11	−8.50	−29.20	64.12	−40.20	−23.24		−37.01
B97	−8.92	−29.18	64.52	−39.07	−30.05		−42.70
B97-D	−8.61	−28.44	63.64	−37.90	−33.58	−0.05	−44.95
wB97	−8.67	−28.79	63.51	−39.79	−22.88		−36.61
wB97X	−8.57	−28.61	63.30	−39.71	−24.61		−38.19
wB97X-D	−8.35	−28.15	62.67	−39.36	−26.08	−0.03	−39.31

close to C_2H_4 decreases while that of the other F atom increases. The small variation of electron density illustrate that there is no obvious electron transfer between C_2H_4 and F_2. In general, the polarization term, which is in agreement with the EDDMs quite well, provides a physically meaningful description for the orbital interaction.

In general, with the help of the EDDM analysis, it is found that for the local and some hybrid functionals, the electron transfer is involved in the total interaction, leading to the positive polarization and large correlation values, whereas for nonlocal functionals with a relatively large portion of exact HF exchange energy, the total interaction is regarded as a vdW interaction.

4. Symmetric Radical Cation Ar_2^+. The GKS-EDA analysis results for the symmetric radical cation Ar_2^+ with the ACCT basis set are shown in Table 7. The experimental binding energy is −30.8 kcal/mol.[101] It is known that the proper description of the interactions in the symmetric radical cation is difficult for DFT functionals, which tend to overestimate the binding energy.[56,102]

By GKS-EDA, the Ar_2^+ binding energy is controlled by the polarization and correlation interaction. The electrostatic interaction is less important. The ΔE^{disp} values of BLYP-D, B97-D, and WB97X-D are very small. All the DFT interaction energies are overestimated. The DFT performance is mainly attributed by the correlation term.

First, the local functionals BLYP and BLYP-D provide the largest binding energies due to the largest correlation energies. With the 0% exact HF exchange portion, M06-L and B97-D provide the overestimated binding energies, smaller than the BLYP and BLYP-D ones by ∼3 kcal/mol. Notice that the ΔE^{corr} values of the M06-L and B97-D are the second largest among all the tested functionals.

Second, for the hybrid GGA/meta-GGA functionals, arising from the exact HF exchange energy, the correlation term becomes smaller, leading to the decrease of the total interaction energies. For example, the B3LYP interaction energy of −42.06 kcal/mol is smaller than the BLYP value of −46.85 kcal/mol, mainly attributed to the smaller correlation term of −29.43 kcal/mol compared to the BLYP value of −35.38 kcal/mol. With the larger exact HF exchange energy involved, B2PLYP describes the total binding energy with −36.90 kcal/mol, better than the B3LYP one due to the smaller correlation and the larger polarization terms.

Finally, for the range-separated functionals except LC-BLYP, attributed by the smaller correlation terms, the total interaction energies are improved. For example, the CAM-B3LYP total interaction energy is −39.66 kcal/mol, smaller than the B3LYP value because of the decreased correlation term. The LC-BLYP correlation value is the largest among these range-separated functionals, resulting in the overestimated binding energy of −43.39 kcal/mol.

5. Active Site of Azurin (PDB 1e5y) in a Solvated Environment. In the active site of the type-1 copper proteins, the Cu cation is coordinated by a cysteine thiolate ligand and two histidine $N^{\delta 1}$ ligands. An axial coordination is provided by a methionine thioether ligand in plastocyanin, amicyanin, pseudoazurin, rusticyanin, and azurin. In azurin, a second axial coordination is provided by a glycine backbone carbonyl oxygen ligand.[103] According to the previous LMO-EDA analysis,[20] the Cu^+-S^- (Cys) is the strongest among these Cu^+−ligand bonds in the active site, showing the largest degree of covalence. The Cu^+-S^- (Cys) and the two Cu−N (His) ligand bonds compose the basic framework of the copper active site. The fourth ligand, methionine, is somewhat far away from the copper cation compared with the cystine and histidine residues. The bond strength of Cu−S (Met) is important for the biomolecular behavior.[104] As discussed by Ryde,[105,106] Solomon,[107] Ando,[108] Corni,[109] and Li,[110] the Cu^+−S (Met) distance is significantly elongated when the B3LYP is employed for optimization. However, the long axial Cu−S (Met) bond in protein environment has not been analyzed quantitatively.

To investigate this ligand interaction, a model molecule consisting 75 atoms shown in Figure 2 is constructed from the geometrical parameters for the basic form of P. a. azurin (PDB 1e5y),[87] which contains the first layer ligands around the Cu^+ cation, including Cys112, His45, Gly46, His117, and Met121. The model molecule is divided into two monomers: one is the Met121 residue with 15 atoms; the other is the remaining part, containing 60 atoms. The functionals B3LYP, M06-2X, B97-D, wB97X-D, CAM-B3LYP, and M11 are employed.

The GKS-EDA analysis results are shown in Table 8. The DFT performance is determined by ΔG^{corr} and ΔG^{disp}. The DFT total interaction energy varies from +5.87 to −6.22 kcal/mol. The ligand interaction belongs to the vdW interaction. The ΔG^{pol} term is small and not the key factor for the ligand bonding. The positive ΔG^{desol} values, varying from 2.67 to 2.94 kcal/mol, illustrate that the interaction is weakened by the protein environment.

dx.doi.org/10.1021/jp500405s | J. Phys. Chem. A 2014, 118, 2531−2542

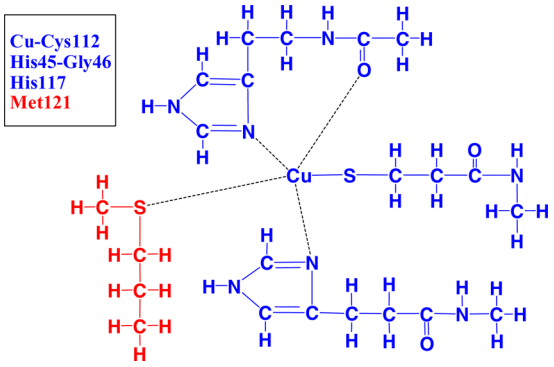

Figure 2. Model molecule for the type 1 copper protein (PDB 1e5y). The red and blue parts are the Met121 residue and the remaining part of the active site, respectively.

The B3LYP interaction energy, 5.87 kcal/mol, is repulsive due to the small ΔG^{corr} value. Despite the fact that CAM-B3LYP provides the larger correlation energy than the B3LYP one, it is still unable to predict the attractive binding energy. As for B97-D, M11, wB97-D, and M06-2X functionals, the Met121 residue can serve as the weak ligand binding to the copper center. As for B97-D and wB97X-D, the attractive interaction energies are attributed by the dispersion terms, −14.73 and −8.87 kcal/mol, respectively. For M11 and M06-2X, their correlation terms are larger than those of B97-D and wB97X-D, compensating the lack of the dispersion interaction. In conclusion, the correlation and dispersion terms are the main factors for this ligand interaction.

E. CONCLUSION

In this paper, a new energy decomposition analysis scheme based on LMO-EDA and EDA-PCM, called GKS-EDA, is presented. Compared to the LMO-EDA scheme, the GKS-EDA scheme shows improvement on the DFT functional adaptability. The GKS-EDA scheme can perform interaction analysis in the gas phase and solvated environments by various DFT functionals, including local, hybrid, double hybrid, rang-separated and dispersion correction functionals, whereas the current version of LMO-EDA cannot work with the rang-separated and dispersion correction functionals. The GKS-EDA interaction terms are defined according to the generalized Kohn−Sham scheme. The exchange, repulsion, and polarization terms are determined by DFT determinant; the correlation term is attributed by the GKS correlation energy; the dispersion term, which is optional for dispersion correction DFT, defined as the difference of the dispersion corrections from monomers to supermolecule without BSSE correction. With the new definition, the GKS-EDA scheme avoids the error of LMO-EDA arising from the separated treatment of E_X and E_C functionals. With the GKS-EDA scheme, the assessment of a series DFT functionals is performed. Some points are highlighted as follows:

1. In most of the examples, the DFT performance is mainly attributed by the correlation interaction. The range-separated DFT functionals, along with M06-2X, providing relatively large correlation energy, tend to mimic the dispersion energy for the hydrogen bonding and vdW interaction. The B2PLYP performs well for the hydrogen bonding and the charge transfer complex, but not suitable for the vdW interactions due to the inadequate description of the correlation interaction.
2. For the $C_2H_4\cdots F_2$ complex, the tested functionals can be regarded as two groups. By the first group, the interaction belongs to electron transfer; whereas by the second group, the interaction can be regarded as vdW interaction. The positive polarization energy by the first group functionals can be well understood by the EDDM, showing the electron transfer from the π bonding orbital of C_2H_4 to the σ_u* orbital of F_2.
3. As for the interaction of the active site in the type 1 copper protein, the long weak ligand of the copper cation provided by Met121 belongs to the vdW interaction, which is weakened by the protein environment.

AUTHOR INFORMATION

Corresponding Author

*P. Su: e-mail, supi@xmu.edu.cn; tel, 86-592-2180413.

Notes

The authors declare no competing financial interest.

ACKNOWLEDGMENTS

This project is supported by the Ministry of Science and Technology of China (No. 2011CB808504), the Natural Science Foundation of China (Nos. 21373165, 21273176, 21120102035), and the Natural Science Foundation of Fujian Province, China (No. 2013J01058).

REFERENCES

(1) Morokuma, K. Molecular Orbital Studies of Hydrogen Bonds. III. C═O···H-O Hydrogen Bond in $H_2CO\cdots H_2O$ and $H_2CO\cdots 2H_2O$. *J. Chem. Phys.* **1971**, *55*, 1236−1244.

(2) Kitaura, K.; Morokuma, K. A New Energy Decomposition Scheme for Molecular Interactions within the Hartree-Fock Approximation. *Int. J. Quantum Chem.* **1976**, *10*, 325−340.

(3) Morokuma, K. Why Do Molecules Interact? The Origin of Electron Donor-Acceptor Complexes, Hydrogen Bonding and Proton Affinity. *Acc. Chem. Res.* **1977**, *10*, 294−300.

Table 8. GKS-EDA Analysis of the Model Molecule for the Active Site of the Type 1 Copper Protein with the 6-31G(d) Basis Set (Azurin, PDB ID 1e5y, kcal/mol)

	ΔG^{ele}	ΔG^{ex}	ΔG^{rep}	ΔG^{pol}	ΔG^{desol}	ΔG^{corr}	ΔG^{disp}	ΔG^{TOT}
B97-D	−12.22	−37.18	58.22	−1.21	2.75	−1.87	−14.73	−6.22
wB97X-D	−11.08	−34.08	53.44	−2.88	2.80	−5.18	−8.87	−5.85
CAM-B3LYP	−11.76	−36.45	56.42	−3.16	2.86	−4.81		3.10
M11	−10.69	−31.63	50.02	−2.57	2.79	−12.75		−4.83
B3LYP	−11.07	−36.80	57.08	−1.90	2.82	−3.35		5.87
M06-2X	−10.84	−33.82	53.01	−2.15	2.67	−14.27		−5.38
B2PLYP	−11.13	−32.68	51.74	−3.47	2.94	−4.32		3.08

(4) Chen, W.; Gordon, M. S. Energy Decomposition Analyses for Many-Body Interaction and Applications to Water Complexes. *J. Phys. Chem.* **1996**, *100*, 14316−14328.
(5) Glendening, E. D.; Streitwieser, A. Natural Energy Decomposition Analysis - an Energy Partitioning Procedure for Molecular-Interactions with Application to Weak Hydrogen-Bonding, Strong Ionic, and Moderate Donor-Acceptor Interactions. *J. Chem. Phys.* **1994**, *100*, 2900−2909.
(6) Bagus, P. S.; Hermann, K.; Bauschlicher, J. C. W. A New Analysis of Charge Transfer and Polarization for Ligand–Metal Bonding: Model Studies of Al_4CO and Al_4NH_3. *J. Chem. Phys.* **1984**, *80*, 4378−4386.
(7) Bagus, P. S.; Illas, F. Decomposition of the Chemisorption Bond by Constrained Variations: Order of the Variations and Construction of the Variational Spaces. *J. Chem. Phys.* **1992**, *96*, 8962−8970.
(8) Stevens, W. J.; Fink, W. H. Frozen Fragment Reduced Variational Space Analysis of Hydrogen-Bonding Interactions - Application to the Water Dimer. *Chem. Phys. Lett.* **1987**, *139*, 15−22.
(9) Mo, Y.; Gao, J.; Peyerimhoff, S. D. Energy Decomposition Analysis of Intermolecular Interactions Using a Block-Localized Wave Function Approach. *J. Chem. Phys.* **2000**, *112*, 5530−5538.
(10) Khaliullin, R. Z.; Cobar, E. A.; Lochan, R. C.; Bell, A. T.; Head-Gordon, M. Unravelling the Origin of Intermolecular Interactions Using Absolutely Localized Molecular Orbitals. *J. Phys. Chem. A* **2007**, *111*, 8753−8765.
(11) Velde, G. T.; Bickelhaupt, F. M.; Baerends, E. J.; Guerra, C. F.; Van Gisbergen, S. J. A.; Snijders, J. G.; Ziegler, T. Chemistry with ADF. *J. Comput. Chem.* **2001**, *22*, 931−967.
(12) Bickelhaupt, F. M.; Baerends, E. J. *Reviews in Computational Chemistry*; Wiley-VCH, Inc.: New York, 2000; Vol. *15*, pp 1−86.
(13) Mitoraj, M. P.; Michalak, A.; Ziegler, T. A Combined Charge and Energy Decomposition Scheme for Bond Analysis. *J. Chem. Theory Comput.* **2009**, *5*, 962−975.
(14) Glendening, E. D. Natural Energy Decomposition Analysis: Extension to Density Functional Methods and Analysis of Cooperative Effects in Water Clusters. *J. Phys. Chem. A* **2005**, *109*, 11936−11940.
(15) Reinhardt, P.; Piquemal, J. P.; Savin, A. Fragment-Localized Kohn-Sham Orbitals Via a Singles Configuration-Interaction Procedure and Application to Local Properties and Intermolecular Energy Decomposition Analysis. *J. Chem. Theory Comput.* **2008**, *4*, 2020−2029.
(16) Ziegler, T.; Rauk, A. On the Calculation of Bonding Energies by the Hartree Fock Slater Method. *Theor. Chem. Acc.* **1977**, *46*, 1−10.
(17) Qin, W.; Paul, W. A.; Yingkai, Z. Density-Based Energy Decomposition Analysis for Intermolecular Interactions with Variationally Determined Intermediate State Energies. *J. Chem. Phys.* **2009**, *131*, 164112−164118.
(18) Steinmann, S. N.; Corminboeuf, C.; Wu, W.; Mo, Y. Dispersion-Corrected Energy Decomposition Analysis for Intermolecular Interactions Based on the BLW and dDXDM Methods. *J. Phys. Chem. A* **2011**, *115*, 5467−5477.
(19) Rajchel, Ł.; Żuchowski, P. S.; Szczęśniak, M. M.; Chałasiński, G. Derivation of the Supermolecular Interaction Energy from the Monomer Densities in the Density Functional Theory. *Chem. Phys. Lett.* **2010**, *486*, 160−165.
(20) Su, P.; Li, H. Energy Decomposition Analysis of Covalent Bonds and Intermolecular Interactions. *J. Chem. Phys.* **2009**, *131*, 014102−014115.
(21) Mo, Y.; Song, L.; Lin, Y. Block-Localized Wavefunction (BLW) Method at the Density Functional Theory (DFT) Level. *J. Phys. Chem. A* **2007**, *111*, 8291−8301.
(22) Wu, Q.; Ayers, P. W.; Zhang, Y. Density-Based Energy Decomposition Analysis for Intermolecular Interactions with Variationally Determined Intermediate State Energies. *J. Chem. Phys.* **2009**, *131*, 164112.
(23) Beyhan, S. M.; Gotz, A. W.; Visscher, L. Bond Energy Decomposition Analysis for Subsystem Density Functional Theory. *J. Chem. Phys.* **2013**, *138*, 094113−094123.
(24) Chen, Y.; Li, H. Intermolecular Interaction in Water Hexamer. *J. Phys. Chem. A* **2010**, *114*, 11719−11724.
(25) Wang, F. F.; Jenness, G.; Al-Saidi, W. A.; Jordan, K. D. Assessment of the Performance of Common Density Functional Methods for Describing the Interaction Energies of $(H_2O)_6$ Clusters. *J. Chem. Phys.* **2010**, *132*, 134303−134308.
(26) Deepa, P.; Kolandaivel, P.; Senthilkumar, K. Hydrogen-Bonding Studies of Amino Acid Side-Chains with DNA Base Pairs. *Mol. Phys.* **2011**, *109*, 1995−2008.
(27) Kumar, R. M.; Baskar, P.; Balamurugan, K.; Das, S.; Subramanian, V. On the Perturbation of the H-Bonding Interaction in Ethylene Glycol Clusters Upon Hydration. *J. Phys. Chem. A* **2012**, *116*, 4239−4247.
(28) Carrazana-García, J. A.; Rodríguez-Otero, J.; Cabaleiro-Lago, E. M. A Computational Study of Anion-Modulated Cation−Π Interactions. *J. Phys. Chem. B* **2012**, *116*, 5860−5871.
(29) Vijay, D.; Sakurai, H.; Subramanian, V.; Sastry, G. N. Where to Bind in Buckybowls? The Dilemma of a Metal Ion. *Phys. Chem. Chem. Phys.* **2012**, *14*, 3057−3065.
(30) Shen, T.; Huang, Z.; Guo, L.; Wang, H. An Ab Initio Study on the Insertion of Radon Atoms into Hypohalous Acids. *Inorg. Chim. Acta* **2012**, *386*, 68−72.
(31) Huang, Z.; Guo, L.; Shen, T.; Ma, L.; Niu, X. Theoretical Study of HKrOX (X = F, Cl, Br and I): Structure, Anharmonic Vibrational Spectroscopy, Stability and Bonding. *Phys. Chem. Chem. Phys.* **2012**, *14*, 8083−8089.
(32) Esrafili, M. D.; Ahmadi, B. A Theoretical Investigation on the Nature of Cl···N and Br···N Halogen Bonds in FArX···NCY Complexes (X = Cl, Br and Y = H, F, Cl, Br, OH, NH_2, CH_3 and CN). *Comput. Theor. Chem.* **2012**, *997*, 77−82.
(33) Camaioni, D. M.; Ginovska-Pangovska, B.; Schenter, G. K.; Kathmann, S. M.; Autrey, T. Analysis of the Activation and Heterolytic Dissociation of H2 by Frustrated Lewis Pairs: NH3/BX3 (X = H, F, and Cl). *J. Phys. Chem. A* **2012**, *116*, 7228−7237.
(34) Steinmann, S. N.; Piemontesi, C.; Delachat, A.; Corminboeuf, C. Why Are the Interaction Energies of Charge-Transfer Complexes Challenging for DFT? *J. Chem. Theory Comput.* **2012**, *8*, 1629−1640.
(35) Durfey, B. L.; Gilbert, T. M. Computational Studies of Lewis Acidities of Tris(Fluorophenyl)-Substituted Boranes: An Additive Relationship between Lewis Acidity and Fluorine Position. *Inorg. Chem.* **2011**, *50*, 7871−7879.
(36) Gao, W.; Feng, H.; Xuan, X.; Chen, L. A Theoretical Study of N−H ··· Π H-Bond Interaction of Pyrrole: From Clusters to the Liquid. *Mol. Phys.* **2012**, *110*, 2151−2161.
(37) Dabbagh, H.; Zamani, M.; Fakhraee, S. The Nature of Resonance and Hyperconjugation for Cyclic β-Silyl Substituted Carbocations: NBO, NRT, EDA, and NMR Studies. *Res. Chem. Intermed.* **2013**, *39*, 2011−2033.
(38) Romero, J.; Reyes, A.; David, J.; Restrepo, A. Understanding Microsolvation of Li^+: Structural and Energetical Analyses. *Phys. Chem. Chem. Phys.* **2011**, *13*, 15264−15271.
(39) Kumar, S.; Pande, V.; Das, A. Π-Hydrogen Bonding Wins over Conventional Hydrogen Bonding Interaction: A Jet-Cooled Study of Indole···Furan Heterodimer. *J. Phys. Chem. A* **2012**, *116*, 1368−1374.
(40) Vacas, T.; Corzana, F.; Jiménez-Osés, G.; González, C.; Gómez, A. M.; Bastida, A.; Revuelta, J.; Asensio, J. L. Role of Aromatic Rings in the Molecular Recognition of Aminoglycoside Antibiotics: Implications for Drug Design. *J. Am. Chem. Soc.* **2010**, *132*, 12074−12090.
(41) Seidl, A.; Görling, A.; Vogl, P.; Majewski, J. A.; Levy, M. Generalized Kohn-Sham Schemes and the Band-Gap Problem. *Phys. Rev. B.* **1996**, *53*, 3764−3774.
(42) Baer, R.; Livshits, E.; Salzner, U. Tuned Range-Separated Hybrids in Density Functional Theory. *Annu. Rev. Phys. Chem.* **2010**, *61*, 85−109.
(43) Becke, A. D. Density-Functional Thermochemistry. III. The Role of Exact Exchange. *J. Chem. Phys.* **1993**, *98*, 5648−5652.
(44) Stephens, P. J.; Devlin, F. J.; Chabalowski, C. F.; Frisch, M. J. Ab Initio Calculation of Vibrational Absorption and Circular Dichroism

Spectra Using Density Functional Force Fields. *J. Phys. Chem.* **1994**, *98*, 11623−11627.
(45) Staroverov, V. N.; Scuseria, G. E.; Tao, J.; Perdew, J. P. Comparative Assessment of a New Nonempirical Density Functional: Molecules and Hydrogen-Bonded Complexes. *J. Chem. Phys.* **2003**, *119*, 12129−12137.
(46) Zhao, Y.; Truhlar, D. The M06 Suite of Density Functionals for Main Group Thermochemistry, Thermochemical Kinetics, Noncovalent Interactions, Excited States, and Transition Elements: Two New Functionals and Systematic Testing of Four M06-Class Functionals and 12 Other Functionals. *Theor. Chem. Acc.* **2008**, *120*, 215−241.
(47) Zhao, Y.; Truhlar, D. G. Exploring the Limit of Accuracy of the Global Hybrid Meta Density Functional for Main-Group Thermochemistry, Kinetics, and Noncovalent Interactions. *J. Chem. Theory Comput.* **2008**, *4*, 1849−1868.
(48) Grimme, S. Semiempirical Hybrid Density Functional with Perturbative Second-Order Correlation. *J. Chem. Phys.* **2006**, *124*, 034108−034116.
(49) Dion, M.; Rydberg, H.; Schröder, E.; Langreth, D. C.; Lundqvist, B. I. Van Der Waals Density Functional for General Geometries. *Phys. Rev. Lett.* **2004**, *92*, 246401−246404.
(50) Lee, K.; Murray, É. D.; Kong, L.; Lundqvist, B. I.; Langreth, D. C. Higher-Accuracy Van Der Waals Density Functional. *Phys. Rev. B* **2010**, *82*, 081101−081104.
(51) Grimme, S.; Antony, J.; Ehrlich, S.; Krieg, H. A Consistent and Accurate Ab Initio Parametrization of Density Functional Dispersion Correction (DFT-D) for the 94 Elements H-Pu. *J. Chem. Phys.* **2010**, *132*, 154104−154119.
(52) Grimme, S. Accurate Description of Van Der Waals Complexes by Density Functional Theory Including Empirical Corrections. *J. Comput. Chem.* **2004**, *25*, 1463−1473.
(53) Jurečka, P.; Černý, J.; Hobza, P.; Salahub, D. R. Density Functional Theory Augmented with an Empirical Dispersion Term. Interaction Energies and Geometries of 80 Noncovalent Complexes Compared with Ab Initio Quantum Mechanics Calculations. *J. Comput. Chem.* **2007**, *28*, 555−569.
(54) von Lilienfeld, O. A.; Tavernelli, I.; Rothlisberger, U.; Sebastiani, D. Optimization of Effective Atom Centered Potentials for London Dispersion Forces in Density Functional Theory. *Phys. Rev. Lett.* **2004**, *93*, 153004−153008.
(55) Iikura, H.; Tsuneda, T.; Yanai, T.; Hirao, K. A Long-Range Correction Scheme for Generalized-Gradient-Approximation Exchange Functionals. *J. Chem. Phys.* **2001**, *115*, 3540−3544.
(56) Vydrov, O. A.; Scuseria, G. E. Assessment of a Long-Range Corrected Hybrid Functional. *J. Chem. Phys.* **2006**, *125*, 234109−234118.
(57) Yanai, T.; Tew, D. P.; Handy, N. C. A New Hybrid Exchange−Correlation Functional Using the Coulomb-Attenuating Method (CAM-B3LYP). *Chem. Phys. Lett.* **2004**, *393*, 51−57.
(58) Chai, J.-D.; Head-Gordon, M. Systematic Optimization of Long-Range Corrected Hybrid Density Functionals. *J. Chem. Phys.* **2008**, *128*, 084106−084115.
(59) Chai, J.-D.; Head-Gordon, M. Long-Range Corrected Hybrid Density Functionals with Damped Atom-Atom Dispersion Corrections. *Phys. Chem. Chem. Phys.* **2008**, *10*, 6615−6620.
(60) Peverati, R.; Truhlar, D. G. Improving the Accuracy of Hybrid Meta-Gga Density Functionals by Range Separation. *J. Phys. Chem. Lett.* **2011**, *2*, 2810−2817.
(61) Hohenberg, P.; Kohn, W. Inhomogeneous Electron Gas. *Phys. Rev.* **1964**, *136*, B864−B871.
(62) Levy, M. Electron densities in search of Hamiltonians. *Phys. Rev. A.* **1982**, *26*, 1200.
(63) Levy, M. Universal Variational Functionals of Electron Densities, First-Order Density Matrices, and Natural Spin-Orbitals and Solution of the V-Representability Problem. *Proc. Natl. Acad. Sci.* **1979**, *76*, 6062−6065.
(64) Parr, R. G.; Yang, W. *Density-Functional Theory of Atoms and Molecules*; Oxford University Press: New York, 1994.
(65) Kohn, W.; Sham, L. J. Self-Consistent Equations Including Exchange and Correlation Effects. *Phys. Rev.* **1965**, *140*, A1133−A1138.
(66) Hayes, I. C.; Stone, A. J. An Intermolecular Perturbation Theory for the Region of Moderate Overlap. *Mol. Phys.* **1984**, *53*, 83−105.
(67) Stone, A. *The Theory of Intermolecular Forces*; Oxford University Press: New York, 2013.
(68) Boys, S. F.; Bernardi, F. The Calculation of Small Molecular Interactions by the Differences of Separate Total Energies. Some Procedures with Reduced Errors. *Mol. Phys.* **1970**, *19*, 553−566.
(69) Ghanty, T. K.; Staroverov, V. N.; Koren, P. R.; Davidson, E. R. Is the Hydrogen Bond in Water Dimer and Ice Covalent? *J. Am. Chem. Soc.* **2000**, *122*, 1210−1214.
(70) Cammi, R.; del Valle, F. J. O.; Tomasi, J. Decomposition of the Interaction Energy with Counterpoise Corrections to the Basis Set Superposition Error for Dimers in Solution. Method and Application to the Hydrogen Fluoride Dimer. *Chem. Phys.* **1988**, *122*, 63−74.
(71) Contador, J. C.; Aguilar, M. A.; Sánchez, M. L.; del Valle, F. J. O. A Theoretical Study of Hydrogen-Bonded Complexes in Solution: Bsse and Decomposition of Interaction Energy. *J. Mol. Struct.: THEOCHEM.* **1994**, *314*, 229−239.
(72) Robert, W. G.; Wojciech, B.; Szczepan, R.; Jerzy, L. Intermolecular Interactions in Solution: Elucidating the Influence of the Solvent. *J. Chem. Phys.* **2004**, *120*, 2802−2813.
(73) Jong, G. T. d.; Bickelhaupt, F. M. Catalytic Carbon−Halogen Bond Activation: Trends in Reactivity, Selectivity, and Solvation. *J. Chem. Theory Comput.* **2007**, *3*, 514.
(74) Fedorov, D. G.; Kitaura, K. Energy Decomposition Analysis in Solution Based on the Fragment Molecular Orbital Method. *J. Phys. Chem. A* **2011**, *116*, 704.
(75) Su, P.; Liu, H.; Wu, W. Free Energy Decomposition Analysis of Bonding and Nonbonding Interactions in Solution. *J. Chem. Phys.* **2012**, *137*, 034111−034115.
(76) Tomasi, J.; Mennucci, B.; Cammi, R. Quantum Mechanical Continuum Solvation Models. *Chem. Rev.* **2005**, *105*, 2999−3094.
(77) Mennucci, B. Polarizable Continuum Model. *Wiley Interdiscip. Rev.: Comput. Mol. Sci.* **2012**, *2*, 386−404.
(78) Barone, V.; Cossi, M. Quantum Calculation of Molecular Energies and Energy Gradients in Solution by a Conductor Solvent Model. *J. Phys. Chem. A* **1998**, *102*, 1995−2001.
(79) Cossi, M.; Rega, N.; Scalmani, G.; Barone, V. Energies, Structures, and Electronic Properties of Molecules in Solution with the C-PCM Solvation Model. *J. Comput. Chem.* **2003**, *24*, 669−681.
(80) Cances, E.; Mennucci, B. Analytical Derivatives for Geometry Optimization in Solvation Continuum Models. I. Theory. *J. Chem. Phys.* **1998**, *109*, 249−259.
(81) Cances, E.; Mennucci, B.; Tomasi, J. Analytical Derivatives for Geometry Optimization in Solvation Continuum Models. II. Numerical Applications. *J. Chem. Phys.* **1998**, *109*, 260−266.
(82) Cossi, M.; Barone, V. Analytical Second Derivatives of the Free Energy in Solution by Polarizable Continuum Models. *J. Chem. Phys.* **1998**, *109*, 6246−6254.
(83) Mennucci, B.; Cammi, R.; Tomasi, J. Analytical Free Energy Second Derivatives with Respect to Nuclear Coordinates: Complete Formulation for Electrostatic Continuum Solvation Models. *J. Chem. Phys.* **1999**, *110*, 6858−6870.
(84) Si, D.; Li, H. Heterogeneous Conductorlike Solvation Model. *J. Chem. Phys.* **2009**, *131*, 044123−044131.
(85) Su, P.; Li, H. Continuous and Smooth Potential Energy Surface for Conductorlike Screening Solvation Model Using Fixed Points with Variable Areas. *J. Chem. Phys.* **2009**, *130*, 074109−074113.
(86) Schmidt, M. W.; Baldridge, K. K.; Boatz, J. A.; Elbert, S. T.; Gordon, M. S.; Jensen, J. H.; Koseki, S.; Matsunaga, N.; Nguyen, K. A.; Su, S. J.; et al. General Atomic and Molecular Electronic-Structure System. *J. Comput. Chem.* **1993**, *14*, 1347−1363.
(87) Nar, H.; Messerschmidt. A. To be Published. DOI: 10.2210/pdb1e5y/pdb. http://www.rcsb.org/pdb/explore/explore.do?structureId=1E5Y.

(88) Rappe, A. K.; Casewit, C. J.; Colwell, K. S.; Goddard, W. A.; Skiff, W. M. UFF, a Full Periodic Table Force Field for Molecular Mechanics and Molecular Dynamics Simulations. *J. Am. Chem. Soc.* **1992**, *114*, 10024−10035.
(89) Lee, C.; Yang, W.; Parr, R. G. Development of the Colle-Salvetti Correlation-Energy Formula into a Functional of the Electron Density. *Phys. Rev. B* **1988**, *37*, 785−789.
(90) Becke, A. D. Density-Functional Exchange-Energy Approximation with Correct Asymptotic Behavior. *Phys. Rev. A* **1988**, *38*, 3098−3100.
(91) Becke, A. D. Density-Functional Thermochemistry. V. Systematic Optimization of Exchange-Correlation Functionals. *J. Chem. Phys.* **1997**, *107*, 8554−8560.
(92) Grimme, S. Semiempirical Gga-Type Density Functional Constructed with a Long-Range Dispersion Correction. *J. Comput. Chem.* **2006**, *27*, 1787−1799.
(93) Zhao, Y.; Truhlar, D. G. A New Local Density Functional for Main-Group Thermochemistry, Transition Metal Bonding, Thermochemical Kinetics, and Noncovalent Interactions. *J. Chem. Phys.* **2006**, *125*, 194101−194118.
(94) Klopper, W.; van Duijneveldt-van de Rijdt, J. G. C. M.; van Duijneveldt, F. B. Computational Determination of Equilibrium Geometry and Dissociation Energy of the Water Dimer. *Phys. Chem. Chem. Phys.* **2000**, *2*, 2227−2234.
(95) Min, S. K.; Lee, E. C.; Lee, H. M.; Kim, D. Y.; Kim, D.; Kim, K. S. Complete Basis Set Limit of Ab Initio Binding Energies and Geometrical Parameters for Various Typical Types of Complexes. *J. Comput. Chem.* **2008**, *29*, 1208−1221.
(96) Curtiss, L. A.; Frurip, D. J.; Blander, M. Studies of Molecular Association in H_2O and D_2O Vapors by Measurement of Thermal Conductivity. *J. Chem. Phys.* **1979**, *71*, 2703−2711.
(97) Seth, M.; Ziegler, T.; Steinmetz, M.; Grimme, S. Modeling Transition Metal Reactions with Range-Separated Functionals. *J. Chem. Theory Comput.* **2013**, *9*, 2286−2299.
(98) Jaszunski, M.; Kochanski, E. Ab Initio SCF Study of the Ethylene + Chlorine Reaction. *J. Am. Chem. Soc.* **1977**, *99*, 4624−4628.
(99) Prissette, J.; Seger, G.; Kochanski, E. Theoretical Study of Some Ethylene-Halogen Molecule (Chlorine, Bromine, Iodine) Complexes at Large and Intermediate Distances from Ab Initio Calculations. *J. Am. Chem. Soc.* **1978**, *100*, 6941−6947.
(100) Zhao, Y.; Truhlar, D. G. Design of Density Functionals That Are Broadly Accurate for Thermochemistry, Thermochemical Kinetics, and Nonbonded Interactions. *J. Phys. Chem. A* **2005**, *109*, 5656−5667.
(101) Wuest, A.; Merkt, F. Potential Energy Curves of Diatomic Molecular Ions from High-Resolution Photoelectron Spectroscopy. I. The First Six Electronic States of Ar_2^+. *J. Chem. Phys.* **2004**, *120*, 638−646.
(102) Zhang, Y.; Yang, W. A Challenge for Density Functionals: Self-Interaction Error Increases for Systems with a Noninteger Number of Electrons. *J. Chem. Phys.* **1998**, *109*, 2604−2608.
(103) Roat-Malone, R. M. *Bioinorganic Chemistry: A Short Course*; John Wiley & Sons, Inc.: New York, 2002.
(104) Chaboy, J.; Díaz-Moreno, S.; Díaz-Moreno, I.; De la Rosa, M. A.; Díaz-Quintana, A. How the Local Geometry of the Cu-Binding Site Determines the Thermal Stability of Blue Copper Proteins. *Chem. Biol.* **2011**, *18*, 25−31.
(105) Ryde, U.; Olsson, M. H. M.; Pierloot, K.; Roos, B. O. The Cupric Geometry of Blue Copper Proteins Is Not Strained. *J. Mol. Biol.* **1996**, *261*, 586−596.
(106) De Kerpel, J. O. A.; Pierloot, K.; Ryde, U. Geometric and Electronic Structure of Co(Ii)-Substituted Azurin. *J. Phys. Chem. B* **1999**, *103*, 8375−8382.
(107) Solomon, E. I.; Szilagyi, R. K.; George, S. D.; Basumallick, L. Electronic Structures of Metal Sites in Proteins and Models: Contributions to Function in Blue Copper Proteins. *Chem. Rev.* **2004**, *104*, 419−458.
(108) Ando, K. Excited State Potentials and Ligand Force Field of a Blue Copper Protein Plastocyanin. *J. Phys. Chem. B* **2004**, *108*, 3940−3946.
(109) Corni, S.; De Rienzo, F.; Di Felice, R.; Molinari, E. Role of the Electronic Properties of Azurin Active Site in the Electron-Transfer Process. *Int. J. Quantum Chem.* **2005**, *102*, 328−342.
(110) Su, P.; Li, H. Protonation of Type-1 Cu Bound Histidines: A Quantum Chemical Study. *Inorg. Chem.* **2009**, *49*, 435−444.